ACS APPLIED MATERIALS & INTERFACES

Research Article

www.acsami.org

# Mussel-Inspired Polydopamine Coated Hollow Carbon Microspheres, a Novel Versatile Filler for Fabrication of High Performance Syntactic Foams

Liying Zhang,[†] Sunanda Roy,[‡] Ye Chen,[‡] Eng Kee Chua,[§] Kye Yak See,[§] Xiao Hu,*[,‡] and Ming Liu*[,†]

[†]Temasek Laboratories, Nanyang Technological University, 50 Nanyang Drive, Singapore 637553, Singapore

[‡]School of Materials Science and Engineering, [§]School of Electrical and Electronic Engineering, Nanyang Technological University, 50 Nanyang Avenue, Singapore 639798, Singapore

Supporting Information

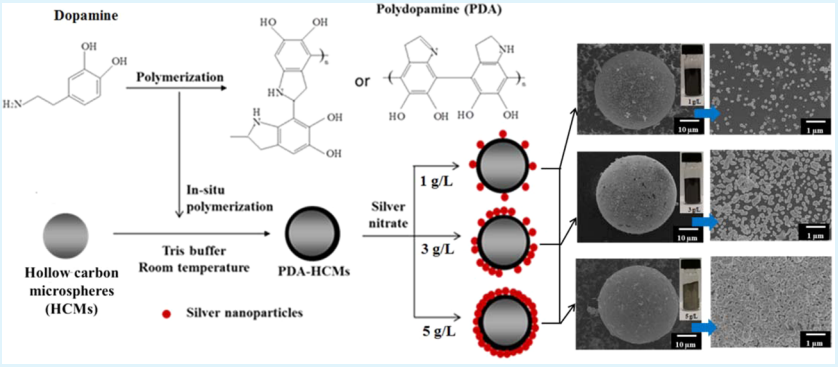


**ABSTRACT:** Syntactic foams, which can be synthesized by mechanical mixing of hollow microspheres with a matrix material, are a special class of lightweight composite materials. Developing of high-performance syntactic foams remains challenges. In this work, a facile and environmentally friendly surface modification method employing polydopamine (PDA) as a surface treatment agent for hollow carbon microspheres (HCMs) was used, aiming to extend the application of syntactic foams to seldom touched areas. The PDA coating was used as a strategy for interfacial interaction enhancement and also as a platform for further metal coating meant for electromagnetic interference (EMI) shielding. The stronger interfacial interaction between microspheres and polymer matrix provided effective interfacial stress transfer, as a result of the syntactic foams with high strength to weight ratio. Furthermore, the PDA coating on HCMs served as a versatile platform for the growth of noble metals on the surface of PDA-HCMs. Silver nanoparticles was grown by PDA medium. The silver coated HCMs (Ag-PDA-HCMs) impacted the complex permittivity of the syntactic foams leading to high EMI shielding effectiveness (SE). The specific EMI SE reached up to 46.3 dB·$cm^3$/g, demonstrated the Ag-PDA-HCMs/epoxy syntactic foam as a promising candidate for lightweight high-performance EMI shielding material.

**KEYWORDS:** *interface, polydopamine, syntactic foam, silver, EMI shielding*

## 1. INTRODUCTION

Since first developed in the early 1960s, syntactic foams were found useful in many areas, such as in aerospace and marine industries.[1,2] They are known to possess high stiffness and excellent compressive strength with low density. Compared with most of other foams, syntactic foam is able to retain the density before and after the curing process.[3] Such property is an advantage during manufacturing process for practical applications.

Syntactic foams can be prepared by mechanical mixing of hollow microspheres (filler) with a matrix material (binder). Different densities and thus microstructures of syntactic foams can be produced by changing the amount of hollow microspheres. The mechanical properties are important parameters for the performance of syntactic foams. To enable their applications, several methods were reported to increase the mechanical properties of syntactic foams. The use of fibrous reinforcements is one of the methods of improving the mechanical properties. The effects of fiber reinforcement in syntactic foams on flexural and compressive properties have already been studied.[4−9] Karthikeyan et al.[4] added 3 wt % of 6 mm glass fibers to the syntactic foam containing hollow glass microspheres, improved the flexural strength by 30%. Our earlier report also demonstrated the role of carbon nanofibers (CNFs) on the mechanical properties of syntactic foams.[9] The flexural strength of the foam increased ∼48.9% with the

Received: June 13, 2014
Accepted: October 6, 2014
Published: October 6, 2014

  

addition of only 1.5 vol % CNFs through effective load transfer from the matrix to CNFs. However, agglomeration and clustering of CNFs at higher concentration hindered the syntactic foam from its optimal performance. The introduction of high volume fractions of nanofillers in syntactic foams resulting in the decrease in the mechanical properties was also observed by other groups.[8,10]

Although the addition of fibers improved the mechanical properties of syntactic foams, it dramatically increased the density of the resulting foam; eventually destroy the main advantage of syntactic foams. Therefore, it is essential to develop a novel method which is able to improve the mechanical properties of syntactic foams while maintain the low density. It is well accepted that the interface between filler and binder plays an important role in determining the mechanical properties of composite materials.[11−13] Similarly, it is expected that an enhancement in the interaction at the hollow microsphere−matrix interface would improve the mechanical properties of syntactic foams without sacrificing their main advantage. In our previous work,[14] we presented a new approach to modify the surface of hollow carbon microspheres (HCMs) in the presence of a coupling agent, glutaric dialdehyde. The treated HCMs were then incorporated into phenolic resin to form the syntactic foam. Results showed excellent improvement in the mechanical properties as a result of effective interfacial adhesion between the HCMs and the phenolic resin. However, the nature of the harsh reaction conditions might cause defects on the surface of the HCMs and the chemicals used for the treatment were environmentally not benign. Moreover, coupling agents are often material-specific and thus lack of efficacy across a broad range of polymer matrices. To overcome the above problems, a more generic and facile functionalization strategy, which is able to generate strong interfacial interactions between the hollow microspheres and a wide variety of polymer matrices, is needed.

Besides mechanical properties, incorporation of functionality in syntactic foams could inspire applications in areas seldom explored before. Electromagnetic interference (EMI) shielding effectiveness (SE) is one of the important functional properties for advanced applications. Note that the weight of materials is one of the major concerns for practical EMI shielding applications; thus, lightweight syntactic foams emerge as an attractive candidate in the field of realistic EMI shielding applications. To date, the studies on the EMI SE of syntactic foams are scarce in the literature and lack of detailed mechanisms. Traditionally, metals are considered to be the materials for EMI shielding applications; however, high density and ease of corrosion restrict their widespread use. Carbon-based materials are often used as conducting fillers in polymer composites, such as carbon nanotube (CNT)[15−19] and CNF,[20,21] but they often suffer from oxidation at high temperature. Compared to metals, the electrical resistivity of carbon-based materials is much higher. Therefore, a greater amount of carbon-based materials is needed to achieve similar EMI shielding effect as metals. This could cause difficulty in fabrication and increase the production cost. The above problems could be solved by applying a thin metal layer on the surface of carbon-based materials. Preparation of metal-coated core−shell composite particles was proposed in order to decrease the amount of metal and the density of metal powder.[22,23] Hence, it can be hypothesized that in the system of syntactic foams, the desired EMI SE coupled with low density could be achieved by the incorporation of metal-coated hollow spheres. Recently, Zheng et al. have reported silver coated hollow glass microspheres and their microwave shielding properties.[24] Although a satisfactory shielding capability was achieved, the coating approach was tedious and not environmentally friendly and the density, as the main parameter for syntactic foams, was not addressed. Therefore, to develop a facile new approach for metal coating on the surface of hollow spheres is essential.

Recently, mussels have been attracting much attention in the research community because of their amazing adhesion ability to various kinds of surfaces.[25] It was confirmed that 3,4-dihydroxy-phenylalanine (precursor of dopamine) was found at high concentrations at the adhesive interfaces between the mussels and the substrates, and is thus responsible for the strong adhesion. Lee et al.[26,27] reported that polydopamine (PDA) layer could be formed on a wide range of materials including polymers, ceramics, noble metals, and semiconductors by self-polymerization of dopamine in an aqueous solution. Yang et al.[28,29] studied the composites which were incorporated with PDA-coated clay and graphene, respectively. It was found that the interfacial PDA layers did not only facilitate the dispersion of the filler, but also strengthen the stress transfer from the polymer matrix to the filler, leading to greatly improved mechanical properties. Moreover, dopamine could be used as a good reducing agent and PDA coating could serve as a versatile platform for metallic coatings. Inspired by these works, we hypothesized that PDA-coated hollow spheres may afford great opportunity to develop high-performance syntactic foams. In this article, we prepared PDA-coated HCMs (PDA-HCMs) and silver coated HCMs (Ag-PDA-HCMs) via a facile surface functionalization step in mild reaction conditions. The PDA-HCMs was incorporated into an epoxy resin to form syntactic foams. Silver was coated on the surface of HCMs with the aim to enhance its functionality, precisely in EMI shielding.

## 2. EXPERIMENTAL SECTION

**Raw Materials.** Hollow phenolic microspheres (BJO-0930) with size ranging from 10 to 50 $\mu$m were purchased from Asia Pacific Microspheres. HCMs were produced by heating the raw hollow phenolic microspheres to 900 °C at a heating rate of 5 °C/min and dewelt for 3 h under constant argon purge.[30] Epoxy epicote 1006 resin and its amine hardener (5:3 by weight) were used as the polymer matrix. Dopamine hydrochloride (99%) and tris(hydroxymethyl)-aminomethane hydrochlorid were purchased from Regent Chemicals Pte Ltd. Polyvinylpyrrolidone (PVP), glucose, silver nitrate, and ammonia were purchased from Sigma-Aldrich. All the chemicals were used as received.

**HCMs Surface Treatment.** The surface of HCMs was ultrasonically cleaned in acetone for 30 min prior treatment. Cleaned HCMs (1 g) were added into 500 mL 10 mM Tris buffer solution (pH 8.5), followed by adding 2.5 g of dopamine hydrochloride. The suspension was mechanically stirred for 6 h at room ambient. The PDA-HCMs were then filtered and washed with deionized (DI) water, followed by freeze-drying. Ag-PDA-HCMs were prepared following the method reported in the previous publications.[31,32] Different concentration of silver nitrate (1, 3, 5, and 10 g/L) was dissolved in 250 mL of DI water followed by dropwise addition of ammonia until the solution became transparent. PDA-HCMs (0.5 g) and 0.5 wt % of PVP were added into the solution and stirred for 15 min. PVP was added as a stabilizing and dispersing agent. The reducing agent glucose (the ratio of glucose to silver nitrate is 2:1) was then added to initiate the reaction. After that, the reaction proceeded under moderate magnetic stirring for 30 min. The Ag-PDA-HCMs were separated by filtration, rinsed by DI water, and dried in a vacuum oven.

**Preparation of Syntactic Foams.** 30 vol % of pristine HCMs, PDA-HCMs, and Ag-PDA-HCMs were added to the epoxy resin, with

**Scheme 1. Schematic Illustration of the Procedure for Preparation of PDA-HCMs and Ag-PDA-HCMs**

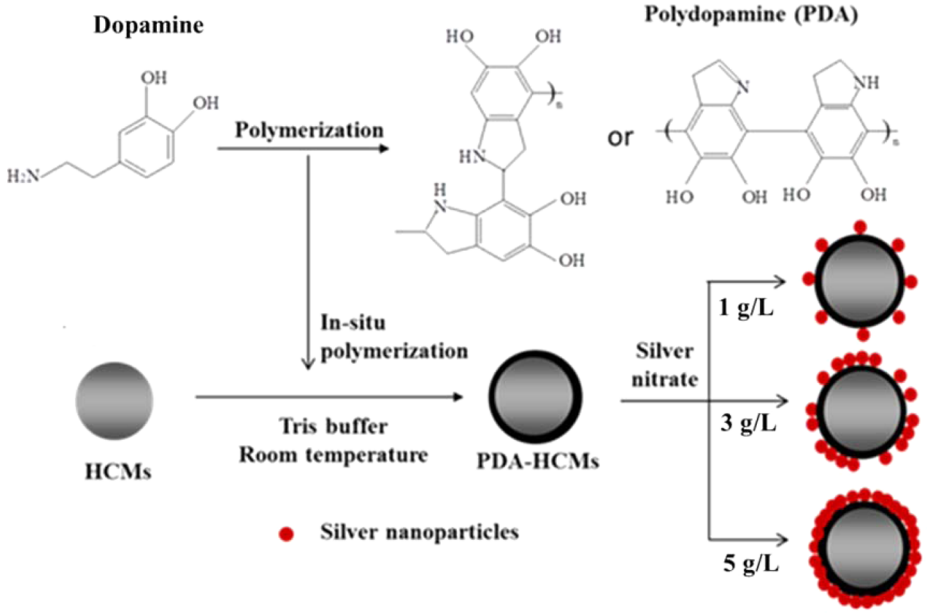


slow stirring to minimize gas bubbles in the resin. The microspheres were added in multiple steps to the resin to avoid agglomeration. The well mixed mixture was poured into an aluminum mold precoated with a silicone release agent. The syntactic foam was then left to cure at room temperature under a constant pressure for 24 h, followed by postcuring at 80 °C for 16 h.

**Characterization.** Fourier transform infrared (FITR) spectra were recorded using a PerkinElmer Instruments Spectrum GX. The thermal stability of different specimens was investigated by a TA Instrument high resolution thermogravimetric analyzer (TGA) Q500 over a temperature range from 25 to 800 °C under nitrogen (60 mL/min) at a heating rate of 10 °C/min. The surface morphologies of specimens were examined by a Jeol JSM 6360 scanning electron microscope (SEM). High magnification surface morphologies were obtained by using a Jeol FESEM 7600F. X-ray diffraction (XRD) patterns were acquired by a Shimadzu X-ray diffractometer (Cu K$\alpha$). The flexural tests were performed using an Instron Tester (Model 5567) according to ASTM Standard D790-07. The compression tests were carried out using an Instron Tester (Model 8516) according to ASTM Standard C365/C365M-05. The EMI SE was measured in the frequency range 8−12 GHz using a PNA-L Network Analyzer (N5230A) measurement system. The samples were fabricated to rectangle plates of 25.4 × 12.7 × 1.5 $mm^3$ to fit the waveguide sample holder. Sample densities in this work were measured using Quantachrome Ultra Foam Gas Pycnometer (Model: 1200e).

## 3. RESULTS AND DISCUSSION

**Dopamine Self-Polymerization on HCMs Surface.** The schematic representation for the preparation of PDA-HCMs is illustrated in Scheme 1. A possible mechanism of dopamine in situ polymerization has already been reported by Xu et al.[33] and Jiang et al.[34] The successful coating of PDA on the surface of HCMs was verified by TGA and SEM as shown in Figure 1. The pristine HCMs showed a weight loss of 5.8% upon heating to 800 °C, indicating the superior thermal stability of the pristine HCMs. The pure PDA showed drastic thermal decomposition around 320 °C and the weight loss was found to be ∼54.6%, whereas the PDA-HCMs showed ∼15.8% weight loss within the same temperature frame. Approximately ∼20.3 wt % of the dopamine loading was found on the HCMs based on the TGA data. The inset SEM images in Figure 1 provided visual confirmation of the PDA coating on HCMs

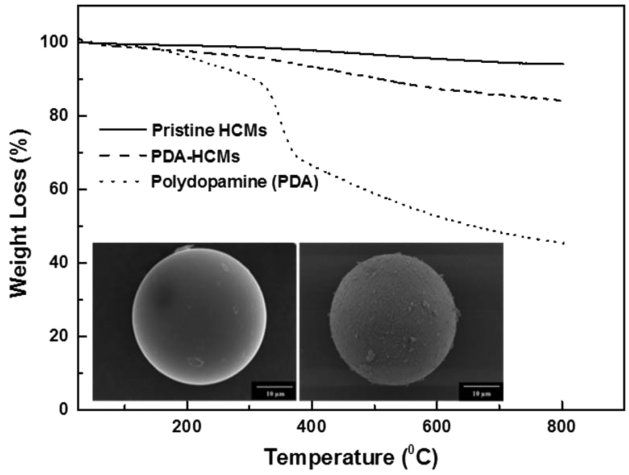


**Figure 1.** TGA curves of pristine HCMs, PDA, and PDA-HCMs in nitrogen atmosphere. Inset SEM images: the pristine HCMs (left) and PDA-HCMs (right).

surface. As shown by the SEM images, the surface of the pristine HCMs was spherical and smooth, while the surface of PDA-HCMs appeared to be much rougher, resulted from the regular grains composed of PDA particles deposited on the surface of pristine HCMs. Figure 2 shows the FTIR spectra of PDA, pristine HCMs and PDA-HCMs. It was found that the same identical bands of PDA appeared at PDA-HCMs, further confirmed the presence of PDA on the surface of the HCMs, indicating the successful coating.

**Mechanical Properties of PDA-HCMs/Epoxy Syntactic Foams.** Figure 3a shows the flexural test stress−strain curves of neat epoxy, the syntactic foam containing 30 vol % of pristine HCMs and PDA-HCMs, respectively. It is clearly shown that when the pristine HCMs were replaced by the PDA-HCMs, the strength of syntactic foams improved dramatically as compared to their counterparts. Moreover, the syntactic foam containing PDA-HCMs exhibited higher Young's modulus and ductility. The increase in mechanical properties was attributed to the presence of PDA, which generated and promoted stronger

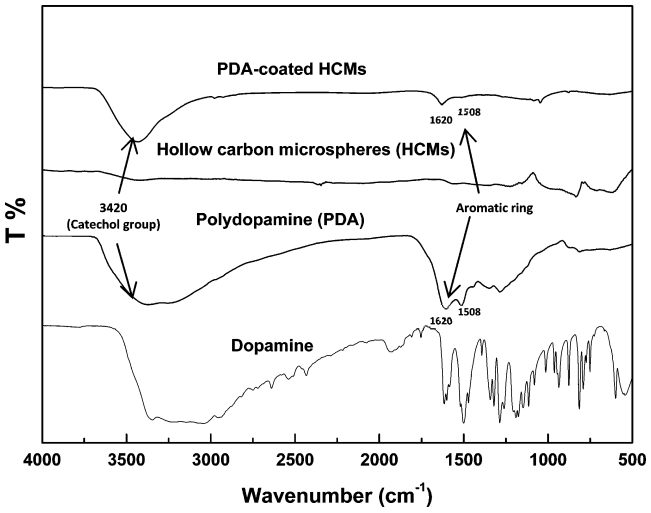


**Figure 2.** FTIR spectra of dopamine, PDA, pristine HCMs, and PDA-HCMs.

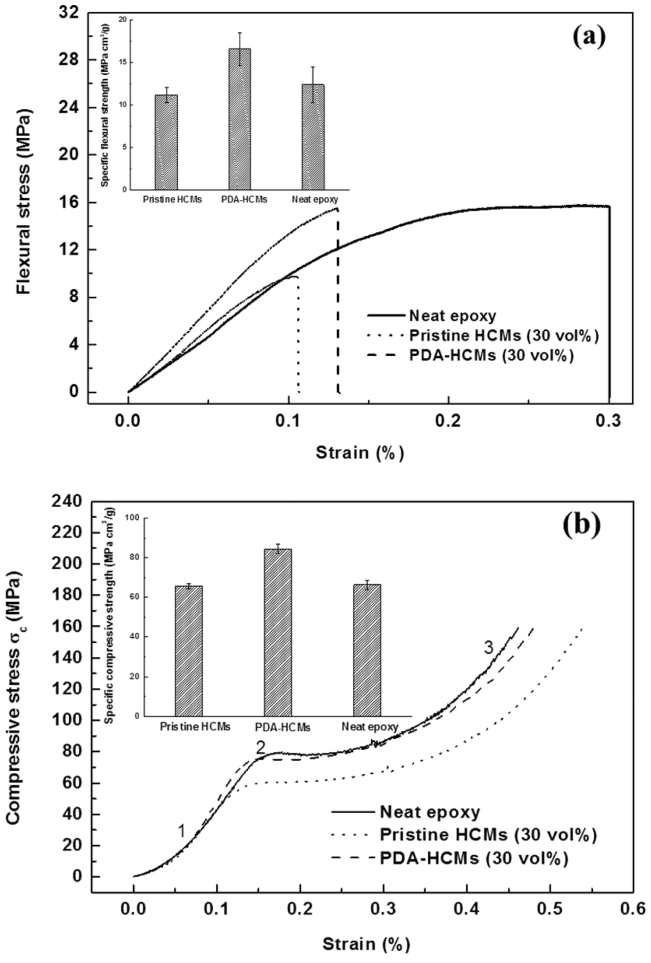


**Figure 3.** Stress–strain curves of (a) flexure and (b) compression for neat epoxy, syntactic foams containing 30 vol % of pristine HCMs and PDA-HCMs. Inset histograms represent the comparison of (a) specific flexural strength and (b) specific compressive strength.

interfacial adhesion between the HCMs and the matrix. Compared with our previous work[14] involving multiple steps of HCMs modification, this facile one-step process was proven to be more efficient and feasible. Figure 3a shows the flexural strength of the syntactic foam containing PDA-HCMs increased by ~37.3% and is comparable to the neat epoxy. This result clearly suggests that PDA coating is an effective approach to enhance the interfacial adhesion strength between fillers and matrix of syntactic foams. The inset bar diagram in Figure 3a compares the specific flexural strength of the specimens, which clearly shows the substantially improved specific flexural strength of the syntactic foam containing PDA-HCMs. The high specific flexural strength was attributed to the increase in interfacial bonding between HCMs and the matrix and simultaneous decrease in density. Figure 3b shows the compression stress–strain curves of neat epoxy, the pristine HCMs, and the PDA-HCMs filled syntactic foams. Similar trend of compression curve has also been reported by other research groups.[1,3,35] For each individual curve, there exist three different regions for the process. Region 1 shows a linear increasing trend in compressive strength, which corresponds to the elastic region of the foam. This region ends when the syntactic foam reaches its compressive yield strength. At the end of the region 1, a slight decrease in strength is observed and yielding occurs, which is the characteristic of region 2. This region corresponds to the implosion of the hollow spheres. When a large number of hollow spheres gets crushed and compacted, further increase in the load results in foam densification and is visible as region 3 of the compression stress–strain curve. One must note that there are three main factors affecting the compressive yield strength of syntactic foams.[14] (1) The introduction of air space from the inside of the hollow spheres. The air space takes up large volume of the matrix, which in turn reduces the compressive yield strength. (2) The interfacial bonding strength between the matrix and the outer surfaces of the hollow spheres. The compressive yield strength improves as long as adequate bonding is maintained. (3) The influence of wall thickness-to-radius ratio, $t/r$, of hollow spheres. The hollow spheres with larger $t/r$ take up more load under compression. In this work, focus was placed on the second factor. As shown in Figure 3b, the compressive yield strength increased when the pristine HCMs were replaced by the PDA-HCMs. When the PDA-HCMs were introduced, the interfacial strength between the epoxy resin matrix and outer surfaces of HCMs increased. These bonded interfaces need to be overcome before the crushing of the HCMs and the occurrence of severe damage, hence improved the compressive yield strength and made it comparable to that of the neat epoxy. The inset bar diagram in Figure 3b shows the specific compressive strength of the specimens. It is observed that the specific compressive strength of the syntactic foam containing the pristine HCMs was comparable to that of the neat epoxy, whereas the specific compressive strength of the syntactic foam comprised of PDA-HCMs was substantially improved by ~28.7% and the value reached to 84.4 MPa·cm$^3$/g. The high specific compression properties were also attributed to the increase in interfacial bonding between HCMs and the matrix and simultaneous decrease in density. The specific flexure and compression properties demonstrated here allow the comparison of performance of the syntactic foam containing PDA-HCMs to other potential composites and foam materials. The enhancement of the mechanical properties due to the presence of PDA in the system of syntactic foams can serve as a model study. Therefore, we believe that the above results would be very useful for guiding future design of composite materials especially for applications where weight is a critical aspect.

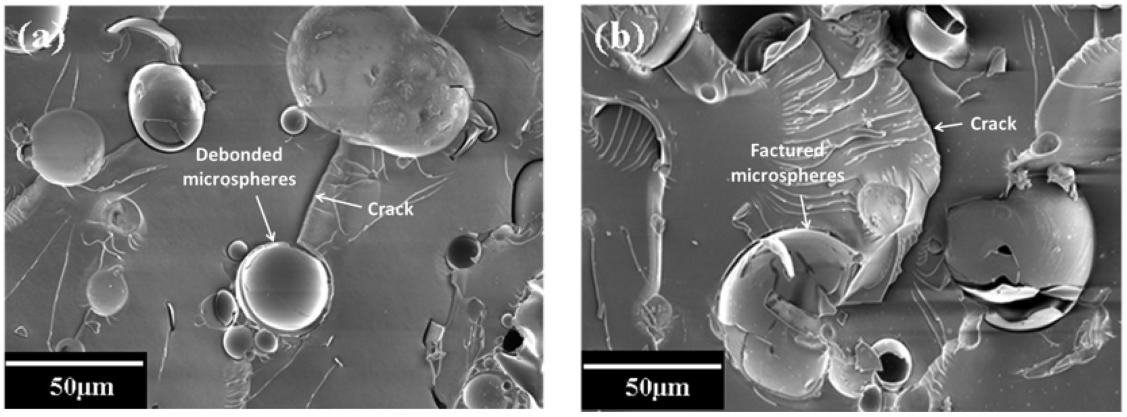


**Figure 4.** SEM images of the fracture surfaces of syntactic foams containing pristine HCMs (a) and PDA-HCMs (b).

In order to illustrate the interfacial adhesion mechanisms, the fracture surfaces of the syntactic foam containing 30 vol % of pristine HCMs and PDA-HCMs were examined by SEM and presented in Figure 4. The foam contains three constituents: the HCMs, the epoxy resin matrix and the interface between HCMs and matrix. The local phenomena include the crack passing through the HCMs, the rupture of the sphere-resin matrix interface and the rupture of the spheres and resin themselves. Figure 4a shows the crack initiated and propagated in the matrix upon loading. The hollow spheres acting as the reinforcement phase divert the crack front propagation. When the crack reaches the interface between the hollow spheres and the matrix, crack deflection occurs and results in the debonding of hollow spheres. The fractured microspheres observed in Figure 4b provided a direct evidence of the hindered crack propagation due to the improved interfacial adhesion between the PDA-HCMs and the matrix. When the crack grows over the interface between the hollow spheres and matrix, extra energy is required to break the adhesion force and to create a new interface. If the interfacial bonding is strong, the crack passes through the spheres causing the spheres to fracture as shown in Figure 4b.

**Silver Coating on PDA-HCMs.** In order to develop the functionality of syntactic foams, we attempted to use the PDA coating as a medium to reduce silver ions and subsequently grow silver nanoparticles on the surfaces of PDA-HCMs. The schematic representation for the preparation of Ag-PDA-HCMs through PDA medium is also illustrated in Scheme 1. The photographs of Ag-PDA-HCMs specimens with different silver content are shown in Figure S1 in the Supporting Information. XRD was performed to ascertain the crystal structure of sliver on the HCMs surface. The XRD pattern for Ag-PDA-HCMs in Figure 5 consists of four distinct characteristic peaks at the $2\theta$ values of 38.2°, 44.4°, 64.5°, and 77.5° corresponding to Ag (111), Ag (200), Ag (220), and Ag (311), respectively. No impurity peak was observed from the XRD spectrum. These results indicated the presence of silver on the surface of HCMs. The morphologies of Ag-PDA-HCMs with different silver content were presented in Figure 6. The collective SEM images of various Ag-PDA-HCMs are shown in Figure S2 in the Supporting Information. It can be seen that the silver nanoparticles increased in size, compactness and continuity with increasing concentration of $AgNO_3$. When the concentration of $AgNO_3$ was 1 g/L, the silver nanoparticles on the spheres surface were discontinuous and sparse (Figure 6a and b). The amounts of silver nanoparticles increased when the

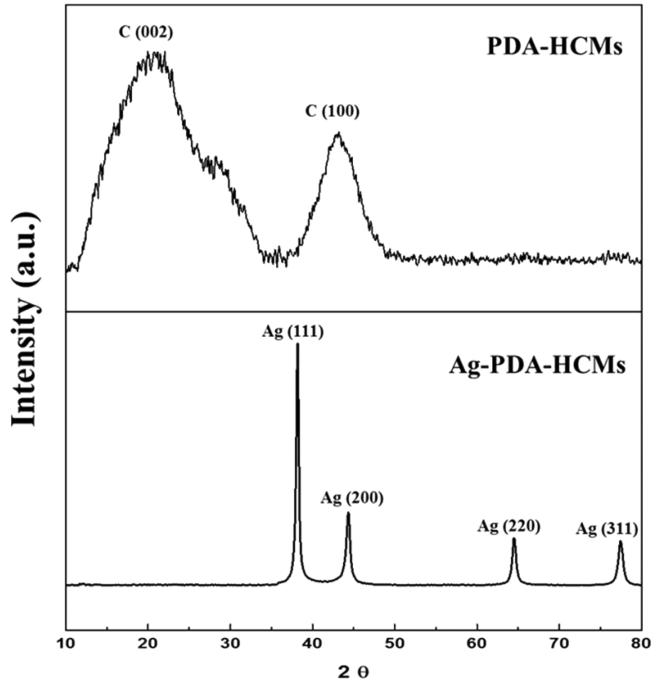


**Figure 5.** XRD patterns of PDA-HCMs and Ag-PDA-HCMs (5 g/L $AgNO_3$).

concentration of $AgNO_3$ increased to 3 g/L. Partially continuous silver nanoparticles were observed (Figure 6c and d). At 5 g/L (Figure 6e and f), a continuous silver layer was formed on the surface of spheres. Further increase in the $AgNO_3$ concentration to 10 g/L (Figure 6g and h), the PDA-HCMs was completely covered with a silver shell and the thickness further increased. The formation of such continuous sliver layer covering the entire spheres impacted the EMI SE of the syntactic foam, which will be studied next.

**EMI SE of Ag-PDA-HCMs/Epoxy Syntactic Foams.** EMI SE of a material is defined as the ratio between incoming power ($P_i$) and outgoing power ($P_0$) of an electromagnetic (EM) wave, SE = 10 log($P_i/P_0$). SE is generally expressed in decibels (dB). The EMI SE of syntactic foam containing Ag-PDA-HCMs with different silver content as a function of frequency is presented in Figure 7a. Note that the densities of the specimens are presented in Table S1 in the Supporting Information and the weight fraction of silver can be converted and applied accordingly afterward. It is observed that the EMI SE increased

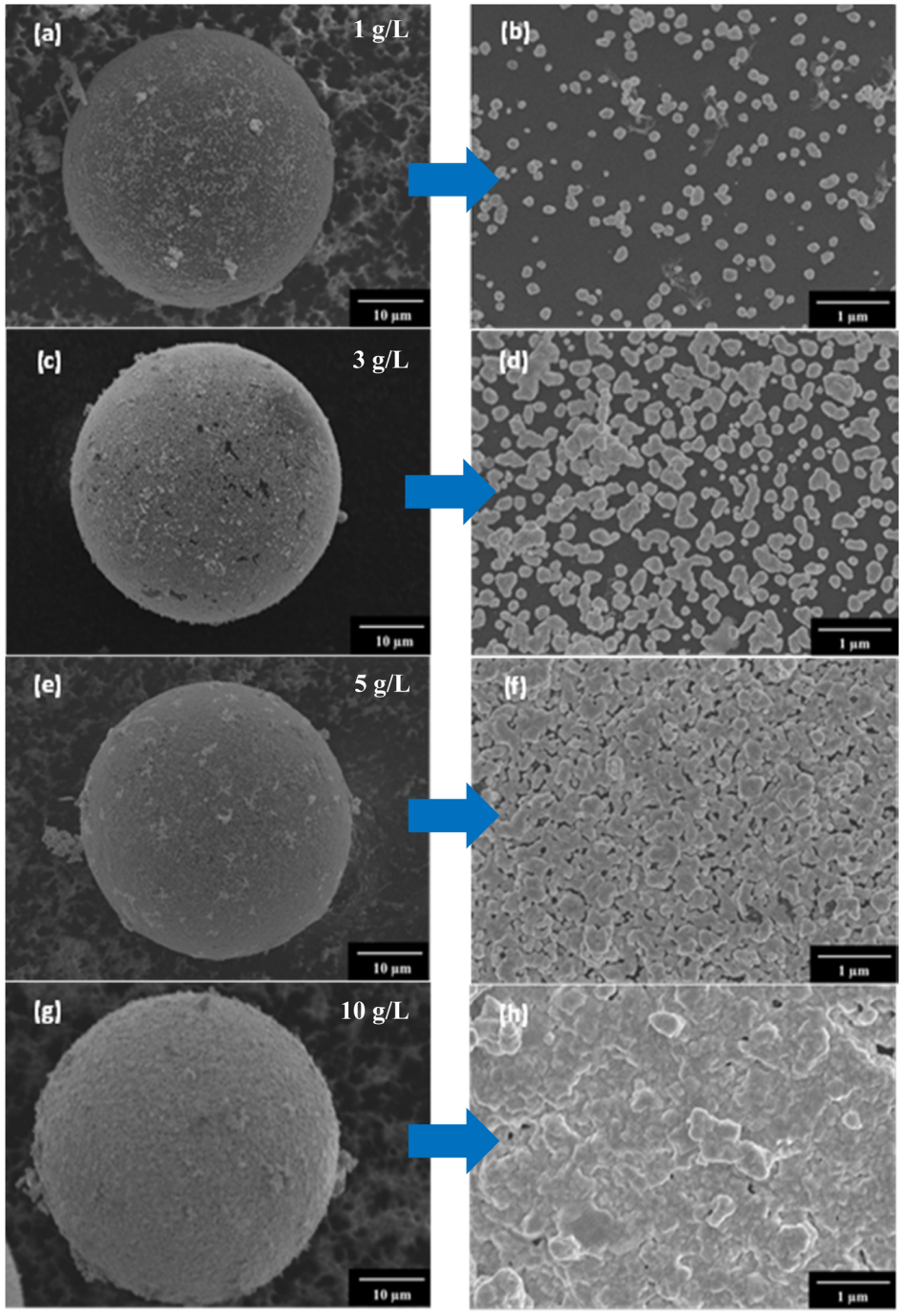


**Figure 6.** SEM images of Ag-PDA-HCMs prepared by different concentration of $AgNO_3$. Right column shows the morphology of the surfaces at higher magnification. (a and b) 1 g/L $AgNO_3$; (c and d) 3 g/L $AgNO_3$; (e and f) 5 g/L $AgNO_3$; (g and h) 10 g/L $AgNO_3$.

with increasing silver content. The average SE of the syntactic foam containing Ag-PDA-HCMs with 28.5 and 30.5 wt % of silver over the frequency range 8−12 GHz was measured to be 49.5 and 60.2 dB, respectively. In general, 20 dB of SE is adequate for most practical applications,[36] and thus, the syntactic foam containing Ag-PDA-HCMs with high silver content surpassed the commercial EMI shielding specifications. Since low density is the main advantage of syntactic foams, the specific EMI SE of our specimens was calculated and compared with other materials. As summarized in Figure 7b, the specific EMI SE increased with increasing silver content and reached up to 46.3 dB·cm$^3$/g, which is much higher than that of CNT/polystyrene foam (33.1 dB·cm$^3$/g),[15] carbon nanofiber/epoxy foam (24.6 dB·cm$^3$/g),[21] and solid copper (10 dB·cm$^3$/g).[37] Recently, Chen et al.[38] reported a lightweight graphene foam of specific EMI SE of 500 dB·cm$^3$/g, the highest specific EMI SE until date. However, compared to syntactic foams, the mechanical properties of the graphene foam is much inferior. Therefore, syntactic foams containing Ag-PDA-HCMs have their outstanding advantages used as high-performance EMI shielding materials. The results presented here allow the use of these materials in areas where mechanical integrity is desired, such as aerospace and automobiles.

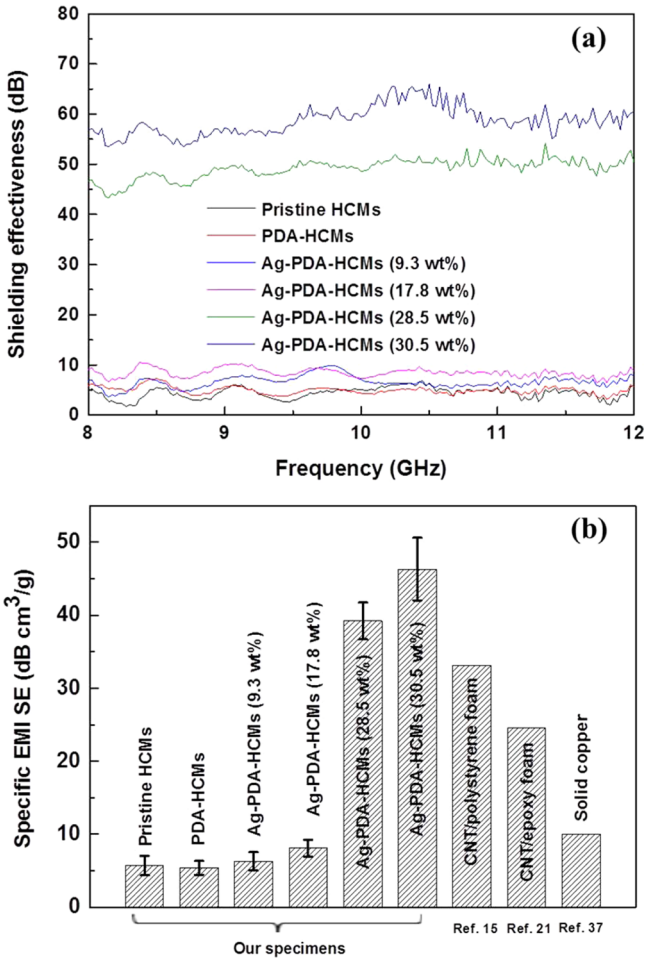


**Figure 7.** (a) EMI SE as a function of the frequency range from 8 to 12 GHz for syntactic foam containing pristine HCMs and Ag-PDA-HCMs with different silver contents. (b) Comparison of the specific EMI SE of different materials with the results in this work.

It is worth noting that the presence of PDA on the HCMs has no obvious effect on the EMI SE of the syntactic foam. As discussed before,[28,29] the interfacial PDA layers did facilitate the good dispersion of the filler resulting in improved mechanical and functional properties. In their cases, the fillers which have high aspect ratio (graphene and clay) tend to aggregate when being dispersed in the polymer resin. The interfacial PDA layers could assist in reduce the agglomeration of fillers. In the system of syntactic foams, the filler used was hollow microspheres, which could be easily dispersed uniformly in the matrix compared to the high aspect ratio fillers, such as CNFs, CNTs, clays, etc. In our case, PDA layers improved the interface interaction but shown little effect on the dispersion of the microspheres, which could cause no significant effect on the EMI SE properties. Hence, silver coating was conducted to improve the EMI SE effect.

We also analyzed the EMI shielding mechanism of syntactic foam containing Ag-PDA-HCMs. When an incident EM wave propagates through a shielding material, the total incident power is the sum of the reflected, absorbed and transmitted powers, as defined by reflectance ($R$), absorbance ($A$), and transmittance ($T$). The $R$, $A$, and $T$ must sum to the value "one", that is, $R + A + T = 1$.[39] The $R$, $A$, and $T$ can be calculated through S-parameters measurement. The schematic proposed EMI shielding mechanisms for a slab of syntactic foam containing Ag-PDA-HCMs is illustrated in Scheme 2. A portion of the wave was reflected and a portion was absorbed when an incident EM wave struck the surface of the specimen. Figure 8a shows the measured $R$, $A$, and $T$ for syntactic foams containing Ag-PDA-HCMs with different silver content at a frequency of 10 GHz. It can be seen that for the specimen with silver below 17.8 wt %, $A \approx R$, indicates that the specimens are both reflective and absorptive to EM radiation in the X-band frequency range. At 28.5 wt % of silver, $A$ reduced to 0.16 and $R$ increased to 0.83. Thus, the contribution of reflection to the total EMI SE is much larger than that from absorption. When the silver content further increased to 30.5 wt %, the more compact and thicker electrical conducting silver layer formed on the surface increased the $R$ to 0.97. This indicated that reflection was the dominant shielding mechanism for the specimen with 30.5 wt % of silver. In order to understand the reasons for EM wave reflection and absorption by shielding material, the intrinsic parameters of the materials, that is, complex permittivity, $\varepsilon_r$ ($\varepsilon_r = \varepsilon' - j\varepsilon''$, where $\varepsilon'$ is the real part

**Scheme 2. Schematic Proposed EMI Shielding Mechanisms for a Slab of Syntactic Foam Containing Ag-PDA-HCMs**

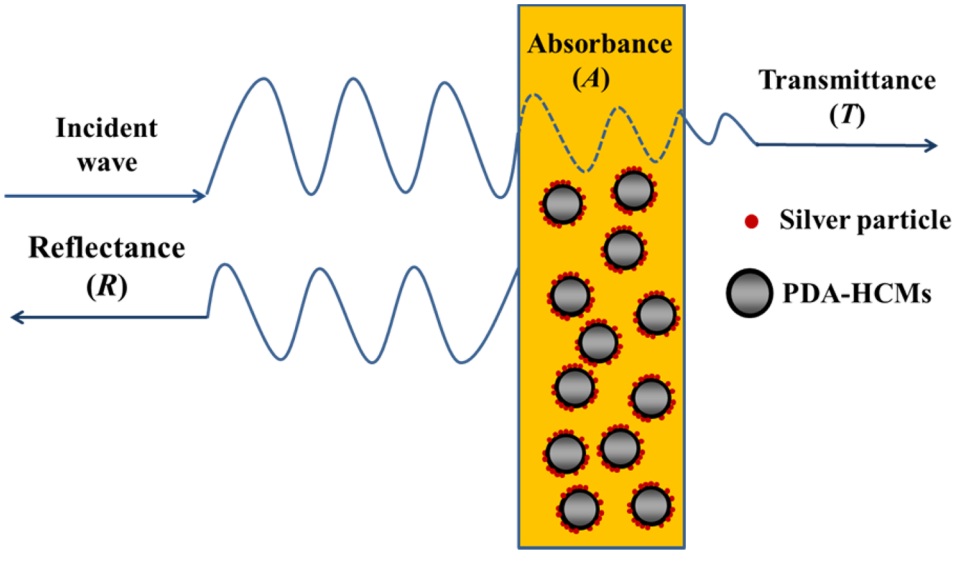

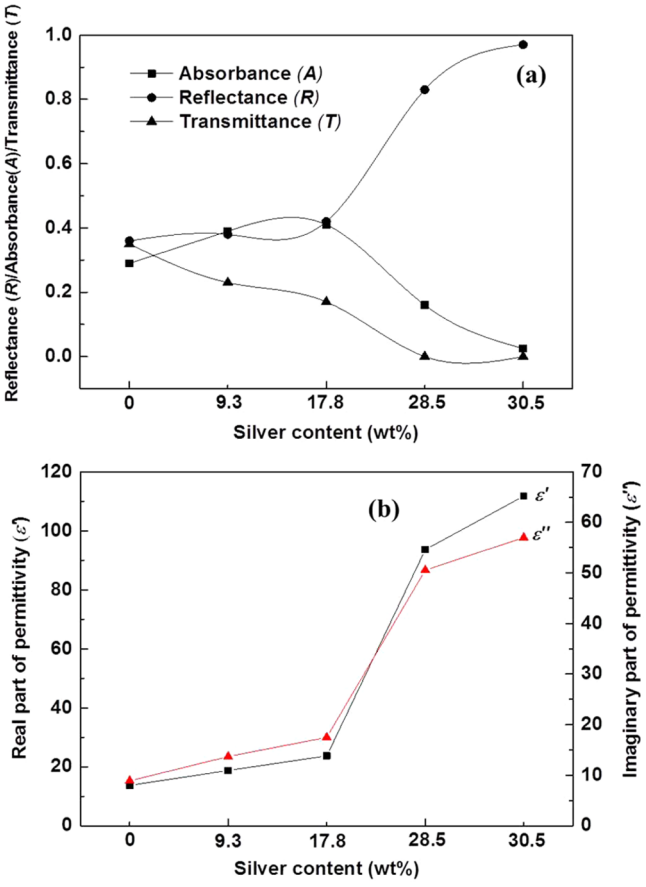


**Figure 8.** (a) Reflectance ($R$), absorbance ($A$), and transmittance ($T$) of EM radiation over syntactic foams containing Ag-PDA-HCMs with different silver content at 10 GHz. (b) Relative complex permittivity of the syntactic foam containing Ag-PDA-HCMs with different silver content at 10 GHz.

and $\varepsilon''$ is the imaginary part) were used for analysis. According to the theory of complex permittivity, when an incident EM wave strikes on the surface of shielding material, the electric field induces two types of electrical currents within the material, that is, the conduction and displacement currents. The conduction currents correspond to the imaginary part of permittivity arises from free electrons and causes high electric loss. The displacement currents which are related to real part of permittivity come from polarization effect. Accordingly, the enhanced polarization effect and electrical conductivity of the shielding material lead to increase both the real and imaginary part of complex permittivity.[40] In this work, $\varepsilon'$ and $\varepsilon''$ can be obtained by using Nicholson-Ross-Weir (NRW) technique through S-parameters.[41] Figure 8b shows the complex permittivity of the syntactic foam containing Ag-PDA-HCMs with different silver content at a frequency of 10 GHz. It is noticed that both $\varepsilon'$ and $\varepsilon''$ increased with increased the silver content, which was ascribed to the effect of enhanced polarization and electric loss of the specimens. For the specimens with higher silver content such as 28.5 and 30.5 wt % of silver, the high permittivity reflected the high electric flux due to the enhanced polarization of electron clouds. Hence, reflection is the main EMI shielding mechanism.

## 4. CONCLUSIONS

In summary, a facile bioinspired coating strategy was proposed to promote strong interfacial bonding between HCMs and epoxy resin. A systemic work was carried out to study the effect of PDA coating on the flexural and the compressive properties of HCMs/epoxy resin syntactic foam. The PDA coating greatly benefited the interfacial interactions between HCMs and epoxy and hence improved the flexural and the compressive properties. The failure mechanisms analysis indicated that the crack was blocked by the good interface between the spheres and the matrix, which in turn caused the fracturing of the spheres, hence improving the overall mechanical properties of the foams. Meanwhile, we also demonstrated that PDA coating can be used to serve as a versatile platform to prepare Ag-PDA-HCMs. The resultant foam containing Ag-PDA-HCMs exhibited high specific EMI SE (46.3 dB $cm^3/g$), which strongly extend the practical applications of syntactic foams. It is expected that the results in this work would be fruitful for guiding future design for syntactic foams and beneficial for special applications.

## ■ ASSOCIATED CONTENT

### Ⓢ Supporting Information

Photograph of Ag-PDA-HCMs prepared by electroless plating with different $AgNO_3$ concentrations; collective SEM images of various Ag-PDA-HCMs; table of the comparison of the density of the specimens. This material is available free of charge via the Internet at http://pubs.acs.org.

## ■ AUTHOR INFORMATION

### Corresponding Authors

*E-mail: ASXHU@ntu.edu.sg.
*E-mail: LIUMING@ntu.edu.sg.

### Notes

The authors declare no competing financial interest.

## ■ ACKNOWLEDGMENTS

The authors acknowledge the support from School of Materials Science and Engineering and Electromagnetic Effects Research Laboratory at Nanyang Technological University on the present work. The authors also express appreciation to Prof. Xuehong Lu, Prof. Linbing Kong, Dr. Ting Sun, and Dr. Xiuzhi Tang for the constructive suggestions and discussions.

## ■ REFERENCES

(1) Bunn, P.; Mottram, J. T. Manufacture and Compression Properties of Syntactic Foams. *Composites* **1993**, *24*, 565−571.
(2) Rizzi, E.; Papa, E.; Corigliano, A. Mechanical Behavior of a Syntactic Foam: Experiments and Modeling. *Int. J. Solids Struct.* **2000**, *37*, 5773−5794.
(3) Wouterson, E. M.; Boey, F. Y. C.; Hu, X.; Wong, S. C. Specific Properties and Fracture Toughness of Syntactic Foam: Effect of Foam Microstructures. *Compos. Sci. Technol.* **2005**, *65*, 1840−1850.
(4) Karthikeyan, C. S.; Sankaran, S. Kishore Influence of Chopped Strand Fibres on the Flexural Behaviour of a Syntactic Foam Core System. *Polym. Int.* **2000**, *49*, 158−162.
(5) Wouterson, E. M.; Boey, F. Y. C.; Hu, X.; Wong, S. C. Effect of Fiber Reinforcement on the Tensile, Fracture, and Thermal Properties of Syntactic Foam. *Polymer* **2007**, *48*, 3183−3191.
(6) John, B.; Nair, C. P. R.; Ninan, K. N. Tensile and Flexural Properties of Glass-Fibre-Reinforced Cyanate Ester Syntactic Foams. *Polym. Polym. Compos.* **2008**, *16*, 431−438.

(7) Nguyen, N. Q.; Gupta, N. Analyzing the Effect of Fiber Reinforcement on Properties of Syntactic Foams. *Mater. Sci. Eng., A* **2010**, *527*, 6422−6428.
(8) Colloca, M.; Gupta, N.; Porfiri, M. Tensile Properties of Carbon Nanofiber Reinforced Multiscale Syntactic Foams. *Composites, Part B* **2013**, *44*, 584−591.
(9) Zhang, L. Y.; Ma, J. Effect of Carbon Nanofiber Reinforcement on Mechanical Properties of Syntactic Foam. *Mater. Sci. Eng., A* **2013**, *574*, 191−196.
(10) Wouterson, E. M.; Boey, F. Y. C.; Wong, S. C.; Chen, L.; Hu, X. Nano-Toughening Versus Micro-Toughening of Polymer Syntactic Foams. *Compos. Sci. Technol.* **2007**, *67*, 2924−2933.
(11) Fu, S.-Y.; Feng, X.-Q.; Lauke, B.; Mai, Y.-W. Effects of Particle Size, Particle/Matrix Interface Adhesion and Particle Loading on Mechanical Properties of Particulate-Polymer Composites. *Composites, Part B* **2008**, *39*, 933−961.
(12) Fang, M.; Wang, K.; Lu, H.; Yang, Y.; Nutt, S. Covalent Polymer Functionalization of Graphene Nanosheets and Mechanical Properties of Composites. *J. Mater. Chem.* **2009**, *19*, 7098−7105.
(13) Roy, S.; Sahoo, N. G.; Cheng, H. K. F.; Das, C. K.; Chan, S. H.; Li, L. Molecular Interaction and Properties of Poly(Ether Ether Ketone)/Liquid Crystalline Polymer Blends Incorporated with Functionalized Carbon Nanotubes. *J. Nanosci. Nanotechnol.* **2011**, *11*, 10408−10416.
(14) Zhang, L. Y.; Ma, J. Effect of Coupling Agent on Mechanical Properties of Hollow Carbon Microsphere/Phenolic Resin Syntactic Foam. *Compos. Sci. Technol.* **2010**, *70*, 1265−1271.
(15) Yang, Y. L.; Gupta, M. C. Novel Carbon Nanotube-Polystyrene Foam Composites for Electromagnetic Interference Shielding. *Nano Lett.* **2005**, *5*, 2131−2134.
(16) Li, N.; Huang, Y.; Du, F.; He, X. B.; Lin, X.; Gao, H. J.; Ma, Y. F.; Li, F. F.; Chen, Y. S.; Eklund, P. C. Electromagnetic Interference (EMI) Shielding of Single-Walled Carbon Nanotube Epoxy Composites. *Nano Lett.* **2006**, *6*, 1141−1145.
(17) Al-Saleh, M. H.; Sundararaj, U. Electromagnetic Interference Shielding Mechanisms of CNT/Polymer Composites. *Carbon* **2009**, *47*, 1738−1746.
(18) Al-Saleh, M. H.; Saadeh, W. H.; Sundararaj, U. EMI Shielding Effectiveness of Carbon Based Nanostructured Polymeric Materials: A Comparative Study. *Carbon* **2013**, *60*, 146−156.
(19) Liu, L.; Das, A.; Megaridis, C. M. Terahertz Shielding of Carbon Nanomaterials and Their Composites—A Review and Applications. *Carbon* **2014**, *69*, 1−16.
(20) Al-Saleh, M. H.; Sundararaj, U. A Review of Vapor Grown Carbon Nanofiber/Polymer Conductive Composites. *Carbon* **2009**, *47*, 2−22.
(21) Zhang, L.; Wang, L. B.; See, K. Y.; Ma, J. Effect of Carbon Nanofiber Reinforcement on Electromagnetic Interference Shielding Effectiveness of Syntactic Foam. *J. Mater. Sci.* **2013**, *48*, 7757−7763.
(22) Yang, J.; Zhang, F.; Chen, Y.; Qian, S.; Hu, P.; Li, W.; Deng, Y.; Fang, Y.; Han, L.; Luqman, M.; Zhao, D. Core−Shell Ag@$SiO_2$@ m$SiO_2$ Mesoporous Nanocarriers for Metal-Enhanced Fluorescence. *Chem. Commun.* **2011**, *47*, 11618−11620.
(23) Mongin, D.; Juve, V.; Maioli, P.; Crut, A.; Del Fatti, N.; Vallee, F.; Sanchez-Iglesias, A.; Pastoriza-Santos, I.; Liz-Marzan, L. M. Acoustic Vibrations of Metal−Dielectric Core−Shell Nanoparticles. *Nano Lett.* **2011**, *11*, 3016−3021.
(24) Huang, Z.; Chi, B.; Guan, J.; Liu, Y. Facile Method to Synthesize Silver Nanoparticles on the Surface of Hollow Glass Microspheres and Their Microwave Shielding Properties. *RSC Adv.* **2014**, *4*, 18645−18651.
(25) Waite, J. H.; Tanzer, M. L. Polyhenolic Substance of Mytilus-Edulis-Novel Adhesive Containing L-DOPA and Hydroxyproline O. *Science* **1981**, *212*, 1038−1040.
(26) Lee, H.; Dellatore, S. M.; Miller, W. M.; Messersmith, P. B. Mussel-Inspired Surface Chemistry for Multifunctional Coatings. *Science* **2007**, *318*, 426−430.
(27) Lee, H.; Lee, B. P.; Messersmith, P. B. A Reversible Wet/Dry Adhesive Inspired by Mussels and Geckos. *Nature* **2007**, *448*, 338−U4.
(28) Yang, L. P.; Phua, S. L.; Teo, J. K. H.; Toh, C. L.; Lau, S. K.; Ma, J.; Lu, X. H. A Biomimetic Approach to Enhancing Interfacial Interactions: Polydopamine-Coated Clay as Reinforcement for Epoxy Resin. *ACS Appl. Mater. Interfaces* **2011**, *3*, 3026−3032.
(29) Yang, L. P.; Phua, S. L.; Toh, C. L.; Zhang, L. Y.; Ling, H.; Chang, M. C.; Zhou, D.; Dong, Y. L.; Lu, X. H. Polydopamine-Coated Graphene as Multifunctional Nanofillers in Polyurethane. *RSC Adv.* **2013**, *3*, 6377−6385.
(30) Zhang, L. Y.; Ma, J. Processing and Characterization of Syntactic Carbon Foams Containing Hollow Carbon Microspheres. *Carbon* **2009**, *47*, 1451−1456.
(31) Wang, W.; Jiang, Y.; Liao, Y.; Tian, M.; Zou, H.; Zhang, L. Fabrication of Silver-Coated Silica Microspheres Through Mussel-Inspired Surface Functionalization. *J. Colloid Interface Sci.* **2011**, *358*, 567−574.
(32) Wang, W.; Cheng, W.; Tian, M.; Zou, H.; Li, L.; Zhang, L. Preparation of PET/Ag Hybrid Fibers via a Biomimetic Surface Functionalization Method. *Electrochim. Acta* **2012**, *79*, 37−45.
(33) Xu, L. Q.; Yang, W. J.; Neoh, K.-G.; Kang, E.-T.; Fu, G. D. Dopamine-Induced Reduction and Functionalization of Graphene Oxide Nanosheets. *Macromolecules* **2010**, *43*, 8336−8339.
(34) Jiang, Y.; Lu, Y. L.; Zhang, L. Q.; Liu, L.; Dai, Y. J.; Wang, W. C. Preparation and Characterization of Silver Nanoparticles Immobilized on Multi-Walled Carbon Nanotubes by Poly(dopamine) Functionalization. *J. Nanopart. Res.* **2012**, *14*.
(35) Gupta, N.; Woldesenbet, E. Kishore Compressive Fracture Features of Syntactic Foams—Microscopic Examination. *J. Mater. Sci.* **2002**, *37*, 3199−3209.
(36) Lundgren, U.; Ekman, J.; Delsing, J. Shielding Effectiveness Data on Commercial Thermoplastic Materials. *IEEE Trans. Electromagn. Compat.* **2006**, *48*, 766−773.
(37) Shui, X. P.; Chung, D. D. L. Nickel Filament Polymer−Matrix Composites with Low Surface Impedance and High Electromagnetic Interference Shielding Effectiveness. *J. Electron. Mater.* **1997**, *26*, 928−934.
(38) Chen, Z.; Xu, C.; Ma, C.; Ren, W.; Cheng, H.-M. Lightweight and Flexible Graphene Foam Composites for High-Performance Electromagnetic Interference Shielding. *Adv. Mater.* **2013**, *25*, 1296−1300.
(39) Huo, J.; Wang, L.; Yu, H. Polymeric Nanocomposites for Electromagnetic Wave Absorption. *J. Mater. Sci.* **2009**, *44*, 3917−3927.
(40) Shi, S.; Zhang, L.; Li, J. Complex Permittivity and Electromagnetic Interference Shielding Properties of $Ti_3SiC_2$/Polyaniline Composites. *J. Mater. Sci.* **2009**, *44*, 945−948.
(41) Nicolson, A. M.; Ross, G. F. Measurement of the Intrinsic Properties of Materials by Time-Domain Techniques. *IEEE Trans. Instrum. Meas.* **1970**, *IM-19*, 377−382.